Thermal annealing effects on structural and magnetic properties of $Fe_{46}Mn_{26}Ga_{28}$ ferromagnetic shape memory alloys

Hui Yang[1, a], Yandong Wang[1, b] and Ke An[2, c]

[1] Key laboratory for Anisotropy and Texture of Materials, Northeastern University, Shenyang 110819, China

[2] Chemical and Engineering Materials Division, Oak Ridge National Laboratory, Oak Ridge, TN 37831, USA

[a] freedomyahu@163.com, [b] ydwang@mail.neu.edu.cn, [c] kean@ornl.gov

Keywords: ferromagnetic shape memory alloys, annealing, γ phase, phase segregation.

Abstract. Annealing plays an important role to adjust structures and properties of ferromagnetic shape memory alloys. Thermal annealing effects on structural and magnetic properties of $Fe_{46}Mn_{26}Ga_{28}$ FSMA have been investigated at different temperatures. Rietveld refinements of neutron diffraction patterns display that the formation of the γ phase in $Fe_{46}Mn_{26}Ga_{28}$ annealed at 1073 K is Fe-rich Ga-poor cubic phase. The atomic occupancies of the alloys are determined due to the neutron's capability of differentiating transition metals. Different annealing treatment introduces magnetic characteristic that is associated with distinctive structural changes in crystal.

1. Introduction

Ferromagnetic shape memory alloys (FSMAs) exhibit both reversible martensitic and ferromagnetic transformations in response to the external magnetic, temperature and stress fields. The shape memory effect that is based on those integrated transformations thus becomes controllable, and it makes FSMAs viable for potential applications as actuators, sensors and electromagnetic devices. Magnetic field induced strain was confirmed in Ni_2MnGa [1,2] and NiMnCoIn [3,4] FSMAs. As a new kind of FSMAs, Fe-Mn-Ga was firstly studied in 2009 exhibiting the martensitic transformation from paramagnetic parent austenite phase to ferromagnetic martensite phase [5]. The Fe-Mn-Ga alloys gradually attracted great interests due to the exhibiting large difference in magnetization between the parent austenite and martensite phases and therefore a large shape memory strain up to 3.6 % [6]. The evolution of the magnetic domain structure in single crystals of a near the composition Fe_2MnGa was observed during phase transition by photoelectron emission microscopy [7]. A recent study of $Fe_{50}Mn_{23}Ga_{27}$ alloy found that the defects-induced local symmetry break suppressed the martensitic transformation without affecting the magnetic ordering [8].

The researches mentioned above are not considered about the annealing effect in Fe-Mn-Ga FSMAs. Actually, annealing treatment is commonly used to tune the structural/magnetic properties in various alloy systems. For example, the martensitic transformation temperature was found to increase with elevating the annealing temperature in $Ni_{55}Fe_{18}Ga_{27}$ [9], and the $Ni_{50.6}Mn_{28}Ga_{21.4}$ microwires [10]. In terms of the magnetic properties under annealing effects, the Curie temperature was increased in $Ni_{50.6}Mn_{28}Ga_{21.4}$ but decreased in $Ni_{51}Fe_{22}Ga_{27}$ [11]. Moreover, the precipitation may form after the thermal treatment to alter the phase structure. The $Ni_{49.5}Mn_{29.3}Ga_{21.2}$ alloy after annealing at 1173 K with presence of γ phase precipitation possesses good ductility and enhanced saturation magnetization [12] and the $Ni_{55}Fe_{18}Ga_{27}$ alloy were observed to have a secondary phase after annealing treatment [13]. Apparently, the properties of the FSMAs have been tuned through the structure modification. However, the specific study of the phase structure evolution and the complex atomic ordering in a ternary Fe-Mn-Ga system under the annealing treatment is essential to understand the structural mechanism of the material behaviors that are closely related to the FSMA performance.

The neutron diffraction is a suitable technique for the phase structure investigation of Fe-Mn-Ga

alloys. The large cross-section of all components make it possible to differentiate multiple phases, and the large penetration depth of neutrons further reflect the behavior of the bulk instead of the surface. Neutron diffraction enables deciphering the site occupancies in the crystal structure of a complex FSMA system, owing to the differentiable scattering contrasts of transition metals elements [14]. Utilizing the advantages of the neutron diffraction for the material structure characterization, in this paper, we select the $Fe_{46}Mn_{26}Ga_{28}$, as the model material to report the significant temperature-dependence of the phase composition and the atomic ordering under the annealing. The annealing effects on the martensitic transformation and the magnetic properties of this FSMA system is to be revealed.

2. Sample preparation and measurements

The polycrystalline button ingots with a nominal composition of $Fe_{46}Mn_{26}Ga_{28}$ were prepared by arc-melting the mixture of the high-purity element metals of Fe, Mn and Ga in a Ti-getter high-purity argon atmosphere, and further fabricated into rod sucked-cast. The ingots were homogenized at 1273 K for 24 hrs and quenched in water and then cut into two sections. One was the homogenized specimen (denoted as Specimen I), the other was then annealed at 1073 K for 2 hrs and quenched in water (denoted as Specimen II). The bulk magnetic properties were measured in using a superconducting quantum interference device magnetometer with heating and cooling rates of 2 $Kmin^{-1}$. The magnetization measurements were performed in the temperature range of 4 K - 300 K with an applied magnetic field up to 6.5 T. The temperature dependence of the magnetization was measured in zero field cooling (ZFC) and in field cooling (FC) modes. The neutron diffraction measurements of Specimen II was collected at the VULCAN instrument at the Spallation Neutron Source (SNS). The neutron diffraction under 2 T magnetic field were measured at the HB2a powder diffractometer at High Flux Isotope Reactor (HFIR), Oak Ridge National Laboratory. The neutron diffraction patterns were analyzed by performing Rietveld refinement using the GSAS software [15] and EXPGUI interface [16], which extract the refined lattice parameters, site occupancies and weight fraction of individual phase.

3. Results

3.1 The influence of annealing on microstructure of $Fe_{46}Mn_{26}Ga_{28}$

The crystal structures were obtained by using Rietveld analysis on the neutron diffraction patterns. For example, Fig. 1 shows the refined patterns of Specimen I and Specimen II at 300 K. The $Fe_{46}Mn_{26}Ga_{28}$ Specimen I has a pure austenite cubic phase (Fmm space group), the lattice parameter of the austenite is ~ 5.85768(2) Å at 300 K. While the face-centered cubic phase and ɣ phase coexisted in the Specimen II at 300 K. The major phase is indexed as a disordered face-centered cubic structure with the lattice parameter a ~ 5.86266(8) Å. The ɣ phase is the cubic phase in the Specimen II which is Fe-rich Ga-poor phase with the lattice parameter a ~3.71100(3) Å. The dissimilar room temperature crystal structures between Specimen I and Specimen II indicate that the high temperature annealing induce the compositional change and the second phase segregated after annealing at 1073 K. The detail of annealing effects on the magnetic transformation will be discussed later.

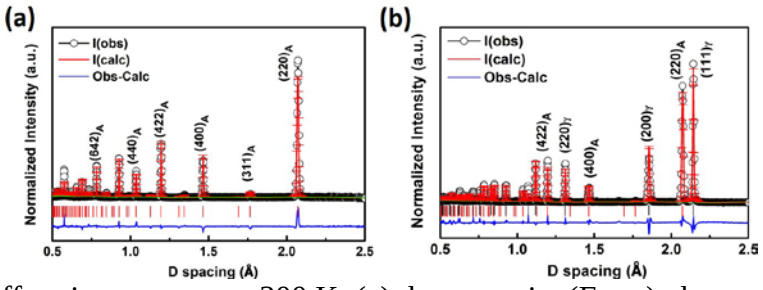

Figure 1. Neutron diffraction patterns at 300 K: (a) the austenite (Fmm) phase at 300 K in Specimen I and (b) the disordered cubic phase and ɣ phase co-exist in Specimen II.

In order to reveal the chemical ordering of Fe, Ga and Mn in the austenite lattice, atom occupancies at the three lattice sites were calculated with Rietveld refinement. In the refinement, the exchange of two elements between two sites were allowed with the full site occupancy constraint and the composition constraint, and the process was repeated throughout the three elements and all three sites until the stable minimum χ^2 was reached. The determined atom occupancies in the parent austenite at room temperature (300 K) is presented in Table 1.

Table 1. Structural details of homogenized specimen I (austenite phase) at 300 K; Fmm space group; a= 5.85768(2) Å. The U_{iso} values of the atoms at the same site are constrained the same.

Atom	Wyckoff	x	y	z	Site occupancy	$100*U_{iso}$
Fe/Mn/Ga	8c	0.25	0.25	0.25	0.636(4)/0.266(4)/0.098(1)	2.19(4)
Fe/Mn/Ga	4b	0.5	0.5	0.5	0.183(4)/0.114(4)/0.703(5)	1.91(2)
Fe/Mn/Ga	4a	0	0	0	0.386(4)/0.393(4)/0.221(5)	1.90(8)

As is shown in Table 1, room temperature Rietveld refinement results show that in the austenite unit cell, the Fe, Ga and Mn atoms mainly occupy the Wyckoff Position 8c (1/4, 1/4, 1/4), 4b (1/2, 1/2, 1/2), and 4a (0, 0, 0), respectively. However, as an off-stoichiometric composition, the structure is not fully ordered because there are multiple species of atoms in each site. The excess Ga atoms (Ga_{Mn}) occupy the Mn sites and some Mn atoms (Mn_{Fe}) shift to the free Fe sites as the result of the defect pair of Ga_{Mn} and Mn_{Fe}. The Fe and Mn atoms also have a certain degree of exchange between 8c and 4a sites. Therefore, the $Fe_{44}Mn_{26}Ga_{28}$ has a partial ordered atomic arrangement in the cubic austenite in Specimen I at 300 K.

Table 2. Structural details of Specimen II at 300 K; Fmm space group; a= 5.86266(8) Å. The U_{iso} values of the atoms at the same site are constrained the same.

Atom	Wyckoff	x	y	z	Site occupancy	$100*U_{iso}$
Fe/Mn/Ga	8c	0.25	0.25	0.25	0.349(7)/0.304(4)/0.345(3)	0.79(2)
Fe/Mn/Ga	4b	0.5	0.5	0.5	0.349(4)/0.350(4)/0.301(2)	0.32(3)
Fe/Mn/Ga	4a	0	0	0	0.410(5)/0.355(3)/0.234(2)	0.45(3)

In Specimen II, there are strong peaks corresponding to the Fmm phase and three weak peaks resulting from the ɣ phase [17,18]. The major phase is indexed as a disordered face-centered cubic structure with the lattice parameter a ~ 3.71100(3) Å (Fig. 2 (a)). The weight fractions of face-centered cubic phase and ɣ phase are 57.069% and 42.904%, respectively, as extracted from the Rietveld refinement using GSAS. The cubic phase is not fully ordered as shown by the atom site occupancy (Table 2) and ɣ phase is a Fe-rich Ga-poor phase which has been reported in similar composition. The dissimilar room temperature crystal structure between Specimen I and Specimen II indicates that the structure transformation temperature may be different due to the compositional change resulting from the formation of the ɣ phase in Specimen II. The detail effect of annealing on the magnetic transformation will be discussed later.

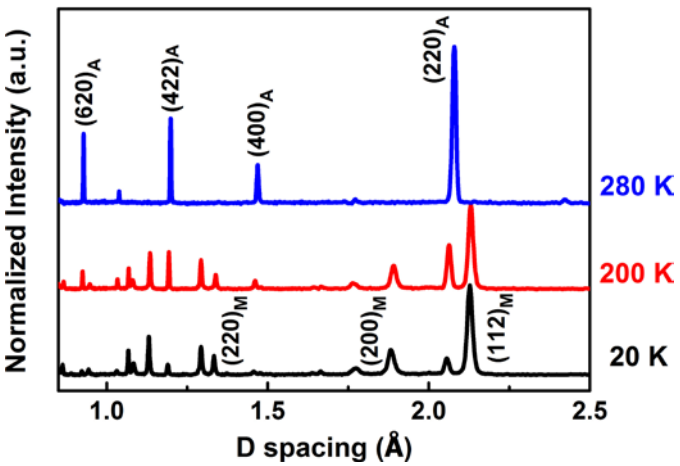

Figure 2. Neutron diffraction patterns of Specimen I heated from 20 K to 280 K, field cooled with an applied magnetic field of 2 T.

In order to understand the structure evolution and the correlation to the magnetic behaviors at the temperature region that we are interested in, the neutron diffraction with applied magnetic field of 2 T was carried out. After field cooling at 2 T, Specimen I shows the martensitic transformation upon heating from 20 K to 280 K as shown Fig. 2. The crystal structure of $Fe_{44}Mn_{26}Ga_{28}$ at 280 K under 2 T magnetic field is Fmm austenite cubic phase, which is same as the structures without the magnetic field. While at 20 K both martensite phase (I4/mmm) and the austenite phase co-exist, the weight fraction of martensite and parent austenite phases at 20 K are 84.255% and 15.745%, respectively. The low-temperature austenite phase lattice monotonically shrinks upon cooling, not showing any anomalous changes. For the tetragonal martensite phase at 20 K, the Fe, Ga and Mn atoms prefer to occupy the Wyckoff Position 4d (0, 1/2, 1/4), 2b (0, 0, 1/2), and 2a (0, 0, 0) in decreasing order as is seen in Table 3. The 4d site is not fully occupied by Fe atoms, with nearly half of it occupied by Mn and Ga atoms. The 2b site is mainly occupied by Ga atoms. The Mn and Fe atoms share most of the 2a site. Similar to the cubic austenite phase, the atoms have different degrees of hybridization at the three transition metal sites.

Table 3. Structural details of Sample I (martensite phase) at 20 K; I4/mmm space group; a= 3.77280(6) Å, c= 7.10859(8) Å. The U_{iso} of all atoms are constrained the same.

Atom	Wyckoff	x	y	z	Site occupancy	$100*U_{iso}$
Fe/Mn/Ga	4d	0	0.5	0.25	0.639(7)/0.180(5)/0.179(9)	0.566(9)
Fe/Mn/Ga	2b	0	0	0.5	0.360(9)/0.449(2)/0.189(9)	0.769(5)
Fe/Mn/Ga	2a	0	0	0	0.360(9)/0.189(9)/0.450(3)	1.617(3)

3.2 Effect of annealing on magnetic properties

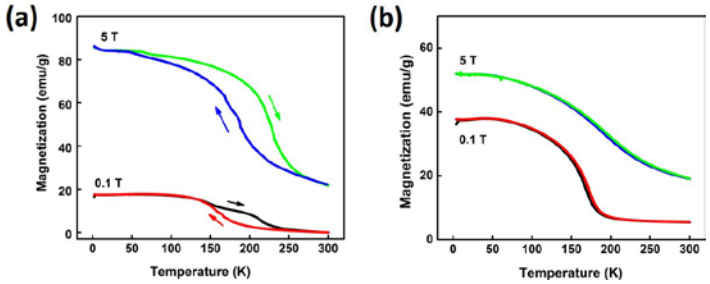

Figure 3. The ZFC and FC thermomagnetization curves (a) Specimen I was measured at 0.1 T and 5 T; (b) Specimen II was measured at 0.1 T and 5 T.

The hysteresis of first order phase transition was observed in Specimen I under magnetic fields as seen in Fig. 3(a). The magnetization of the Specimen I at 5 K is 17.4 emu/g at 0.1 T and 85.3 emu/g at 5 T. According to the results of previous studies of $Fe_{50}Mn_{22.5}Ga_{27.5}$, the magnetization at 5 K in 5 T magnetic field is about 94 emu/g, and the magnetization of $Fe_{43}Mn_{28}Ga_{29}$ at 4.2 K in the same magnetic field is about 83 emu/g [5,6]. This behavior corresponds to a coupled magneto structural phase transition between the ferromagnetic martensite and paramagnetic austenite, which indicates the chemical compositions affect the magnetic properties on Fe-Mn-Ga alloys. Correspondingly, there is no hysteresis first order phase transition displayed in Specimen II under magnetic fields (Fig. 3(b)). It indicates that the Specimen II has no first order phase transition i.e. martensitic transformation occur in the temperature range from 4 K to 300 K.

It should be noted that the magnetization measured under the magnetic field of 0.1 T in Fig. 3(a) demonstrates two marked changes in the slope at heating process and only one change at cooling process in Specimen I. The anomaly slope in heating curve at ~ 160 K can be ascribed to the Curie temperature. It is consistent with $Fe_{72-x}Mn_xGa_{28}$ which showed that in the system [8].

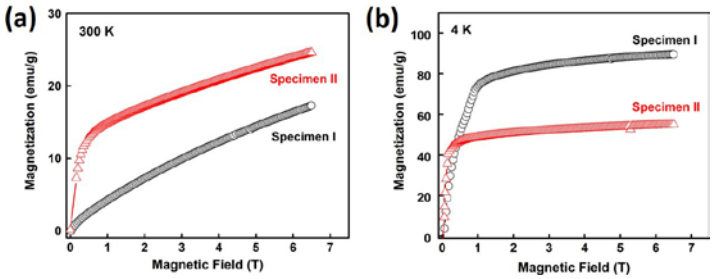

Figure 4. Magnetic field dependence of the magnetization of Specimen I and II measured from 0 T to 6.5 T (a) the magnetization curves at 300 K; (b) the magnetization curves at 4 K.

The magnetization curves of the Specimens at 300 K and 4 K are shown in Fig. 4(a) and (b), respectively. In both temperatures, the saturated magnetization agree with the results in the M(T) data in Fig. 3. At 300 K, Specimen I that is a pure austenite phase shows a linear behavior with increasing magnetic field, as it is paramagnetic (Fig. 4 (a)). The behavior in Specimen II is different from the behavior in Specimen I. The increase in magnetization may be due to the coexistence of ɣ phase, which manifests ferromagnetic at room temperature. Based on the current experimental results, one cannot distinguish the contributions from the two cubic phases or conclude the mechanism for the ferromagnetism. Nevertheless, it is indicated that the ferromagnetism in Fe-Mn-Ga system has significant sensitivity to the rearrangement of different species of atoms in the Fmm cubic lattice.

4. Discussion

Based on the results of the magnetic properties, one can observe the distinct difference in the two specimens. In Specimen I (homogenized at 1273 K), the magnetization at 5 T shows an obvious onset of ferromagnetism in cooling and decay to the paramagnetic phase in heating. The large hysteresis behavior of the magnetization suggests a first-order phase transition that can be correlated to the reversible austenite to martensite structural transition in response to the temperature change under the external magnetic field. Above 250 K, Specimen I becomes paramagnetic completely. The result of the thermomagnetization curve Specimen I is supported by the neutron diffraction results with an applied magnetic field showing the structural phase transitions at temperatures when bulk magnetic phase transitions were observed. Fig. 3 suggests that in Fe-Mn-Ga system, the change of magnetic properties between ferromagnetic and paramagnetic phases is correlated with a similarly reversible structural transformation.

In contrast to Specimen I, the formation of the disordered face-centered cubic ɣ phase in Specimen II (annealed at 1073 K) causes the composition segregation and no hysteresis of first order phase transition in the range from 4 K to 300 K. In Specimen II, the magnetization gradually increases as the temperature goes down towards 5 K, without showing any anomalous behavior. The disappearance of thermal hysteresis should be due to the introduction of the ɣ phase. The possible reason may be attributed to the ɣ phase may bring the local variations in composition of the specimen. Therefore, considering the presence of the amount of ɣ phase which disorders the microstructure of the specimen hinders the structural transition, one may control the martensitic transformation temperatures by tuning the phase composition via the purposive annealing. The structural change may further impact the thermomagnetization behavior of the Fe-Mn-Ga alloy. Moreover, the change in the atomic composition and distribution in the lattice sites also alters the ferromagnetism of the material. This follows from the fact that ɣ phase and disordered cubic phases are ferromagnetic at 300 K, different from the paramagnetic austenite phase as in Specimen I.

When the temperature decreases to 4 K, the paramagnetic austenite phase in Specimen I mostly transforms to the ferromagnetic martensite phase. The martensite phase dominates the magnetization at the low field, and it leads to much higher saturated magnetizations at 4 K in Specimen I (Fig. 4(b)). The existence of the ferromagnetic ɣ phase in Specimen II is the possible reason for the discrepancy from Sample I at the saturation, which is consistent with the situation at

300 K. Moreover, one can see that the magnetization of Specimen II reached saturation at a lower applied magnetic field than that of Specimen I, and the ɣ phase is also thought to be responsible for that. This agrees with the fact that the disordered cubic Fmm lattice in Specimen II has no the structure transformation toward a martensite lattice after the atomic rearrangement during the phase segregation.

As the results of the quenching, dislocations may be expected besides the observed structure changes. But the quantities or dislocation density are expected to comparable and will not show distinctive changes of the magnetic behaviors that is discussed in the following. If significant different amount of dislocations developed in each specimen, the neutron diffraction patterns would show different peak broadenings, which is, however, not observed obviously. Therefore, we believe the magnetic properties are associated more with the distinctive structural changes.

5. Conclusion

In summary, the annealing effects on the structures and magnetic properties in $Fe_{46}Mn_{26}Ga_{28}$ were investigated. The annealing at different temperatures on Fe-Mn-Ga alloys introduces changes in phase structures and magnetic properties. Annealing at 1073 K leads to the disappearance of the first order phase transition in comparison to the as homogenized at 1273 K specimen, which could be ascribed to the formation of the amount of ɣ phase, which is Fe-rich Ga-poor disordered cubic phase by using Rietveld refinement. Furthermore, one can optimize the material composition to attain advanced FSMA by annealing at a temperature that controls the formation of ɣ phase. In addition, there is no structural transformation and display ferromagnetic behavior in the temperature range from 4 K to 300 K.

Acknowledgements

The H.Y. thanks China Scholarship Council for the financial support during the visit to University of Tennessee, TN, SNS, ORNL and National Basic Research Program of China (2012CB619405). Neutron scattering experiments were carried out at SNS and HFIR which are national user facilities sponsored by the Scientific User Facilities Division, Office of Basic Energy Sciences (BES), U.S. Department of Energy. Material fabrication (H. Bei) was supported by the Materials Science and Engineering Division, Office of Sciences, Basic Energy Sciences (BES), U.S. Department of Energy. The authors thank Dr. A. Huq at SNS and Ms. K. Andrews at HFIR for the technical support of the neutron experiments.

References

T. Sakon, K. Otsuka, J. Matsubayashi, et al. Magnetic properties of the ferromagnetic shape memory alloys $Ni_{50+x}Mn_{27-x}Ga_{23}$ in magnetic fields, Materials, vol. 7 (2014) p. 3715-3734.

[1]. Z. H. Nie, D. Y. Cong, D. M. Liu, et al. Large internal stress-assisted twin-boundary motion in Ni_2MnGa ferromagnetic shape memory alloy, Appl. Phys. Lett. vol. 99 (2011) p. 141907.

[2]. A. S. Turabi, H. E. karaca, H. Tobe, et al. Shape memory effect and superelasticity of NiMnCoIn metamagnetic shape memory alloys under high magnetic field, Scripta Mater. vol. 111 (2016) p. 110-113.

[3]. S. Rios, I. Karaman, X. Zhang, Crystallization and high temperature shape memory behavior of sputter-deposited NiMnCoIn thin films, Appl. Phys. Lett. vol. 96 (2010) p. 173102.

[4]. T. Omori, K. Watanabe, R. Y. Umetsu, et al. Martensitic transformation and magnetic field-induced strain in Fe–Mn–Ga shape memory alloy, Appl. Phys. Lett. vol. 95 (2009) p. 082508.

[5]. W. Zhu, E. K. Liu, L. Feng, et al. Magnetic-field-induced transformation in FeMnGa alloys, Appl. Phys. Lett. vol. 95 (2009) p. 222512.

[6]. Y. V. Kudryavstev, N. V. Uvarov, V. N. Iermolenko, et al. Electronic structure, magnetic and optical properties of Fe_2MnGa Heusler alloy, Acta Mater. vol. 60 (2012) p. 4780-4786.

[7]. T. Ma, X. Liu, M. Yan, et al. Suppression of martensitic transformation in $Fe_{50}Mn_{23}Ga_{27}$ by local symmetry breaking, Appl. Phys. Lett. vol. 106 (2015) p. 211903.

[8]. H. J. Yu, X. T. Zu, H. Fu, et al. Effect of annealing and heating/cooling rate on the transformation temperatures of NiFeGa alloy, J. Alloy. Compd. vol. 470 (2009) p. 237-240.

[9]. M. F. Qian, X. X. Zhang, L. S. Wei, et al. Effect of chemical ordering annealing on martensitic transformation and superelasticity in polycrystalline Ni–Mn–Ga microwires, J. Alloy. Compd. vol. 645 (2015) p. 335-343.

[10]. K. Oikawa, T. Omori, R. Kainuma, et al. Effects of annealing on martensitic and magnetic transitions of Ni–Ga–Fe ferromagnetic shape memory alloys, J. Magn. Magn. Mater. vol. 272 (2004) p. 2043-2044.

[11]. K. Pushpanathan, R. Chokkalingam, M. Mahenadan, Martensitic Transformation and Microstructure of Ni-Mn-Ga Magnetic Shape Memory Alloy, Mater. Manuf. Process, vol. 28 (2013) p. 72-78.

[12]. J. Font, J. Muntasell, R. Santamarta, et al. Effect of ageing in Ni–Fe–Ga ferromagnetic shape memory alloys, Mater. Sci. Eng. A vol. 438 (2006) p. 919-922.

[13]. H. Yang, Y. Chen, H. Bei, et al. Annealing effects on the structural and magnetic properties of off-stoichiometric Fe-Mn-Ga ferromagnetic shape memory alloys, Mater. Des. vol. 104 (2016) p. 327-332.

[14]. A. C. Larson and R. B. von Dreele, General structure analysis system (GSAS) LAUR, Los Alamos National Laboratory, New Mexico, 2004.

[15]. B. H. Toby, EXPGUI, a graphical user interface for GSAS, J. Appl. Crystallogr. vol. 34 (2001) p. 210-213.

[16]. Y. Kim, S. J. Lee, W. B. Han, et al. Structure and magnetic properties of low-temperature annealed Ni-Mn-Al alloys, J. Appl. Phys. vol. 113 (2013) p. 17B102.

[17]. W. Maziarz, Structure changes of Co–Ni–Al ferromagnetic shape memory alloys after vacuum annealing and hot rolling, J. Alloy. Compd. vol. 448 (2008) p. 223-226.